Tailor Made Concrete Structures – Walraven & Stoelhorst (eds)
© 2008 Taylor & Francis Group, London, ISBN 978-0-415-47535-8

Shear carrying capacity of Ultra-High Performance Concrete beams

Josef Hegger & Guido Bertram
Institute of Structural Concrete at RWTH Aachen University, Aachen, Germany

ABSTRACT: Ultra-High Performance Concrete (UHPC) is a high-tech material opening new opportunities especially for slender constructions. Within the collaborative research project "Sustainable Building with Ultra High Performance Concrete (UHPC)" supported by the German Research Foundation (DFG) design models for pretensioned beams have been developed at the Institute of Structural Concrete at RWTH Aachen University. Several tests were performed to investigate the bond anchorage and the shear carrying behavior of prestressed concrete beams made of UHPC with or without web openings.

1 INFLUENCE OF THE ANCHORAGE BEHAVIOR ON SHEAR RESISTANCE

The prestressing force above the support is essential to calculate the shear resistance. A decisive contribution of the shear carrying capacity arises from arch action as presented in figure 1. When the anchorage length is shorter than the support overhang, the full prestressing force is available to intensify arch action. The vertical support reaction corresponds with the prestressing and the arch action. Prestressing forces, which have to be transferred in front of the support line, do not contribute to the arch action.

To investigate the anchorage behavior pull-out test and small beam tests were performed. Pretensioned T-beams were fabricated to test the anchorage length and the shear carrying capacity.

2 CONCRETE MIXTURE

All specimen were fabricated with the concrete mix presented in table 1. Merely the fiber type and ratio were varied.

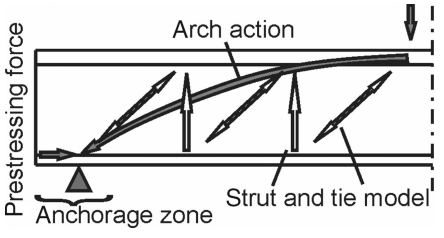

Figure 1. Principle of arch action with corresponding prestressing force.

3 ANCHORAGE BEHAVIOR

3.1 *Pull-out test*

In table 2 an overview of the pull-out tests is given. A total of 72 tests were performed. The main test parameters were the fiber ratio, the specific concrete cover, the concrete strength (age) and the strand diameter. Because of the high bond stresses, short embedment lengths between 25 and 50 mm were chosen. Each batch contains three tests with three different lateral strain stages (0%, 50%, 100%). Figure 2 shows the sequences of the pull-out tests. Three strands have been prestressed inside a testing rig. Then, the specimens were concreted. After a hardening period of three days the first three tests have been conducted. Afterwards, the prestressing force was decreased about 50% and further three tests were preformed. Finally, the last tests were accomplished with full release (100%), which means full lateral strain of the strand.

Table 1. Concrete mix.

Mix/fiber ratio [% p.v.] material	M0 2.5%	M1 0.9%	M7 1.04%	MR w/out
Cement CEM I	650	660	660	666
Silica fume	177	180	180	181
Quartz powder	456	463	463	467
Sand 0.125–0.5 mm	354	360	359	363
Basalt 2–8	598	606	606	612
Steel fiber 9.0/0.15	194	–	–	–
Steel fiber 17.5/0.15	–	70	–	–
Steel fiber 13.0/0.16	–	–	39	–
Steel fiber 6.0/0.15	–	–	42	–
Water	158	161	160	162
Superplasticizer	31	32	32	32

Table 2. Parameters of the pull-out tests (72 tests).

Test	Concrete mix	Cover c/d_p	Age [d]	Strands 0.5”	Strands 0.6”	Number [–]
PO1-3	M1	4.4	3		×	3 × 3
PO4-6	M0	4.4	3		×	3 × 3
PO7-9	M7	4.4	3		×	3 × 3
PO10-15	M1	1.5–2.5	3		×	6 × 3
PO16-18	M1	5.5	3	×		3 × 3
PO19-21	M1	4.4	14		×	3 × 3
PO22-24	MR	4.4	3		×	3 × 3

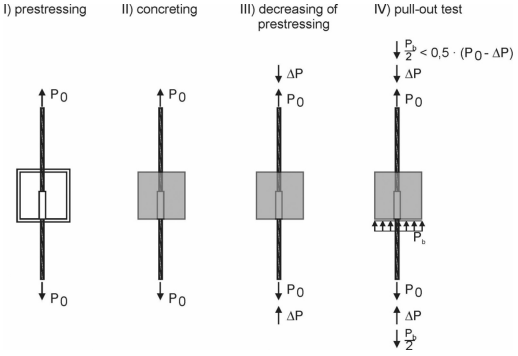

Figure 2. Fabrication and test sequences of pull-out tests.

The diagram in figure 3 indicates, that the fiber ratio has no significant influence within the tested range. With a compressive strength of 100 N/mm² at an age of three days a bond strength of 30 N/mm² was achieved with full lateral strain (100% release of prestressing). Without presenting theses curves in the diagram, 20 N/mm² with 50% release and about 12 to 14 N/mm² without a change of the prestressing force were achieved independent from the fiber ratio.

The variation of the concrete cover showed no effect on the bond strength when the prestressing remains unchanged. A release of 50% led to a reduction of the bond stresses of about 10 to 15%. When the full lateral strain was preset, visible splitting cracks appeared below a specific concrete cover of $c/d_p = 2.5$. This means, the transferred bond stresses were reduced about 10 to 30% according to the existing concrete cover (figure 4).

3.2 *Tests to investigate the transfer length*

The main targets of these 10 tests were to determine the minimum dimensions of the concrete cross section to avoid splitting cracks and to investigate the transfer length of the specimens which remained uncracked. Specimens with two strands were chosen to investigate

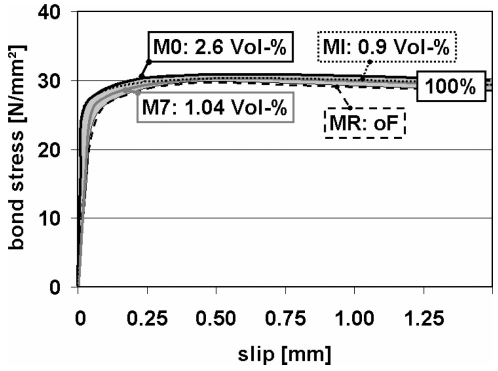

Figure 3. Influence of the fiber ratio on the bond slip behavior of the test batches PO1 to PO9, PO22–PO24 when prestressing was released 100%.

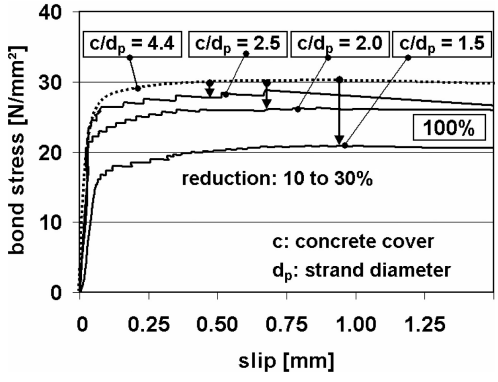

Figure 4. Influence of the concrete cover on the bond slip behavior of the test batches PO10 to PO12 when prestressing was released 100%.

the minimum concrete cover (figure 5). Four strands were required to test the minimum spacing between the strands. The concrete mix M1 with 0.9% p.v. was used for all beams and the concrete age at the day of the tests was always three days. Further details and results are given in Hegger & Bertram (2008a).

Similar to the pull-out tests, the specimens were fabricated in a rig. The strands were already prestressed at the time of concreting. After the hardening period the prestressing was released in steps of 20%. At each load stage the concrete strains were measured along the longitudinal axis of the specimen. This way, the transfer of prestressing can be derived from the strain differences. In addition, the slip at the end of the specimen was measured continuously with displacement transducers.

Splitting cracks in the area of the transfer zone are hardly visible, especially when steel fibers are added to the concrete. However, the development of splitting cracks can be spotted by a sudden slip increase. The

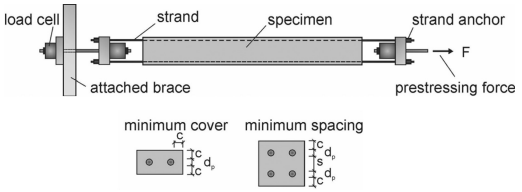

Figure 5. Test setup to determine the transfer length as well as the minimum dimensions.

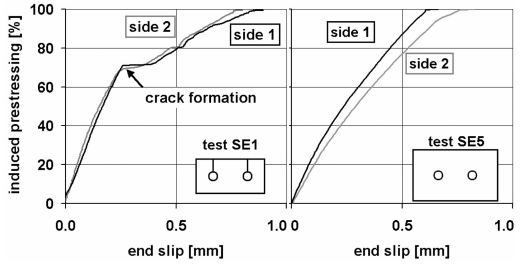

Figure 6. End slip of the strands, SE1 with cracks, SE5 without visible cracks.

left diagram of figure 6 indicates, that the specimen SE1 with a specific concrete cover of $c/d_p = 1.5$ started cracking when 70% of the prestressing was induced. Due to the splitting crack the stress depending part (hoyer-effect) diminished leading to a higher slip. SE2 with $c/d_p = 2.0$ cracked at 95%. Only when the specific concrete cover amounts at least $c/d_p = 2.5$ the full prestressing was feasible without visible cracks as indicated by the continuous load-slip behavior in the right diagram of figure 6. Compared to HSC a reduction of the minimum concrete cover cannot be accomplished. Most likely, the splitting stresses arose simultaneously due to the higher bond stresses.

Nevertheless, the transfer length is shorter compared to NSC or even HSC when cracks were avoided as shown in the diagram of figure 7. In these cases the measured transfer length amounts to 25 cm on average. The transfer length was extended when splitting cracks appeared, anyhow the strands have been anchored after 40 to 50 cm (SE1).

3.3 *Calculative bond model*

So far, several investigations have been performed on the anchorage behavior of strands, amongst others by den Uijl (1992), Stocker & Sozen (1969), Nitsch (2001) and Bülte (2008). Generally, the bond stresses can be divided into three parts (figure 8):

- a constant part caused by the basic friction, also called the rigid-plastic bond behavior.

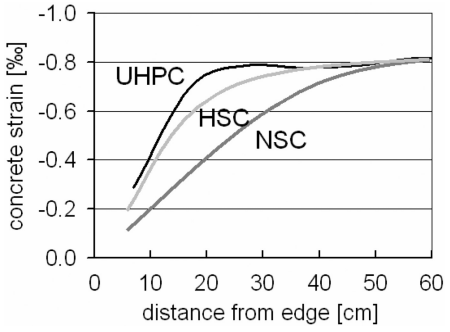

Figure 7. Concrete strain at the end of the test compared to HSC and NSC.

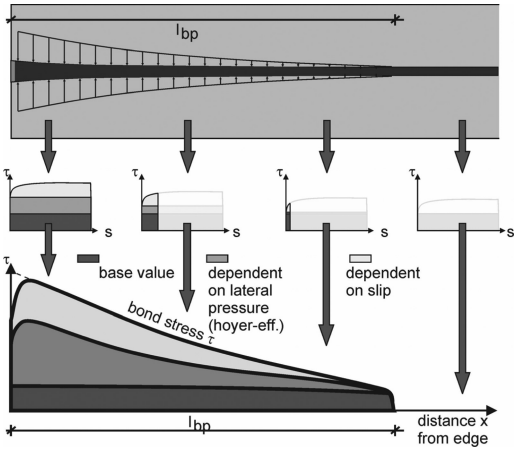

Figure 8. Schematical stress distribution along the transfer length of strands l_{bp}.

- a stress dependent part which is based on the hoyer-effect and which increases with the transfer of pretensioning.
- and a slip dependent part which is also independent of the prestressing. This effect can be explained by the "lack of fit" which results from the geometry of the strands which is not completely uniform.

On the basis of the results from the pull-out tests a stress-slip relation can be derived, which takes into account the lateral strain and the slip. As demonstrated by Bülte (2008) the local bond strength can be translated to components by using the bond differential equation system. Therefore, the differential equation for steel bars from Nitsch (2001) has been upgraded to a formulation for strands prestressed with pretensioning:

$$\frac{d^2 s_p(x)}{dx^2} = \frac{1}{E_p} \cdot \left(f(s_p;\sigma_p) \cdot \frac{U_p}{A_p} \left(1 + \alpha_p \cdot \rho_p\right) \right) \quad (1)$$

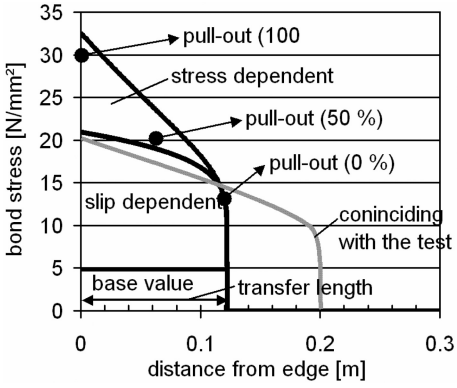

Figure 9. Comparison of theoretical and experimental transfer length for test SE3.

Using any stress-slip relation the stresses as well as the slip in the transfer zone can be calculated. The resulting theoretical transfer length can be checked by the measured one in the beam tests. The test SE3 without visible cracks was used to examine the applicability of the bond law according to Nitsch (2001). The theoretical transfer length was calculated by using the local bond stresses of the pull-out tests. The theoretical transfer length $l_{bp,cal} = 12.2$ cm in figure 9 as well as the theoretical slip $s_{cal} = 0.37$ mm (without diagram) fall below the experimental values ($l_{bp,exp} \gg 20$ cm/ $s_{exp} \gg 0.48$ mm).

In principle, these differences may have the following reasons:

- The bond law, which was derived for normal and high strength concrete, cannot be transferred to UHPC without adequate modification. Especially the proportion between compressive strength and bond strength may have a significant influence.
- A damage of the specimen may have occurred, even though it was not visible. This means, that microcracks developed but the steel fibers prevented the crack growth. Nevertheless, the stress dependent part of the bond stresses was decreased. The cracks in the other specimen with smaller concrete cover were hardly visible, too.

In figure 9 the results of the pull-out tests are marked. The bond stresses are insignificantly lower than the theoretical values of the curve, i.e. the approached bond law according to Nitsch (2001) leads to results in the right range. Furthermore, the experimental transfer length is too long compared to high strength concrete. Invisible crack development seems to be the main reason. Therefore, further tests with enlarged concrete cover will be added on.

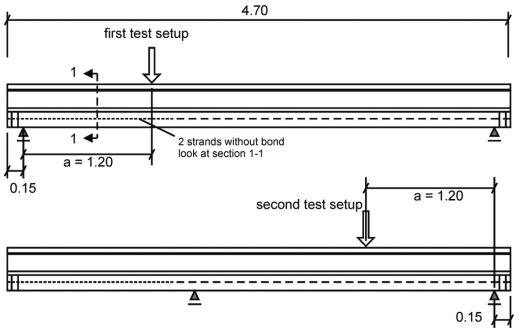

Figure 10. Test setup of T1–T4 (solid beams, T4 without debonded strands and a = 1.40 m).

4 SHEAR TESTS

4.1 *Parameters of the shear tests*

An overview of the conducted shear test program is given in table 3. Due to the specific loading (Figure 10) two tests with different prestressing grades could be performed on one beam. The first test is indicated with "a" and the second with "b". To avoid an anchorage failure, two stirrups Ø6 were arranged behind the support. A considerable enhancement of the overhang is not expedient because the rising arch action influences the shear carrying capacity more than in common practice. A size of 15 cm was appointed for all shear tests. The specific concrete cover was $c/d_p = 2{,}5$ according to the small tests. The lower chord was pretensioned with nine 0.5" strands, each with a prestressing of 125 kN (figure 11). Two of the middle strands were debonded on one side of the beam (T1–T3). This way, two different ratios of prestressing could be realized in one beam. All other parameters as the effective depth maintained the same. To investigate the influence of the shear slenderness, the forth beam was tested with $a/d = 3.8$ (T4a) and 4.4 (T4b).

4.2 *Results of the shear tests without openings*

Generally, the shear tests showed a very stiff load bearing behavior due to the high prestressing. In figure 12 the load-deflection diagrams for three beam tests with different fiber ratios are presented.

The comparison of the load deflection curves of T1b, T2b and T3b in figure 4 as well as the ultimate shear forces in table 3 indicate the effectiveness of the steel fibers as shear reinforcement. Even 0.9% p.v. of steel fibers led to an increase of 80% and an amount of 2.5% p.v. even of 177% in comparison to T2b without fibers. The shear bearing capacity of T3a was even higher than the bending resistance. To prevent bending failure, the test was aborted. The flexural strength Rf of the concrete compositions with 0.9%

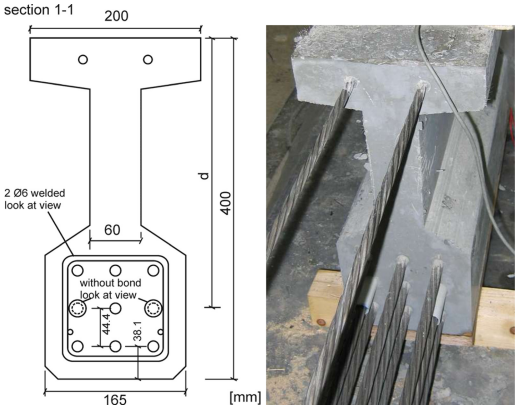

Figure 11. Cross section of T1–T4 (T4 without debonded strands).

Table 3. Parameters of the shear tests.

Test	Concrete mix	Slenderness a/d	Strands with openings	
			Bond/total	No./a1*
T1a	M1	3.8	7/9	–
T1b	M1	3.8	9/9	–
T2a	MR	3.8	7/9	–
T2b	MR	3.8	9/9	–
T3a	M0	3.8	7/9	–
T3b	M0	3.8	9/9	–
T4a	M1	3.8	9/9	–
T4b	M1	4.4	9/9	–
T6a	M1	3.8	9/9	1/0.5d
T6b	M1	3.8	9/9	1/1.0d
T7a	M1	3.8	9/9	1/1.5d
T7b	M1	3.8	9/9	1/2.0d

* a1 : distance between support and opening

fiber content (T1, T4) and 2.5% (T3) were almost in the same range. But the flexural strength without fibers (T2) was considerably reduced. The flexural strength was determined with three point bending tests (prism dimension: 4 cm × 4 cm × 16 cm).

In test T1b (0.9% p.v.) first shear cracks developed at a shear load of 245 kN which led to a decrease in initial stiffness. Further cracks appeared continuously while loading. The ultimate shear load of 267 kN was reached at a deflection of 9 mm. The main failure cracks were declined between 20° and 24° with spacings from 2 to 3 cm. As expected, the ultimate shear force of T1b was superior to T1a due to the higher prestressing (table 4). Two main failure cracks in T1a were declined 20° and 22°. Entirely different, the second beam without steel fibers failed without any indication. The crack pattern of the failure cracks was similar but there was a sudden failure after the first crack developed. When 2.5% steel fibers were

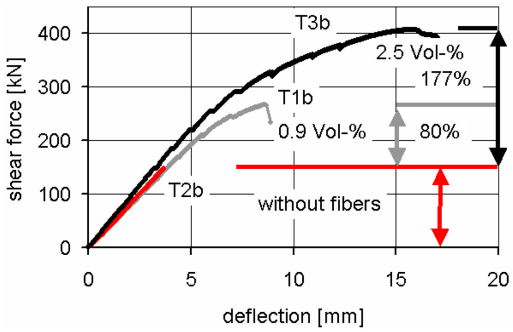

Figure 12. Comparison of the load bearing behavior with different fiber ratios.

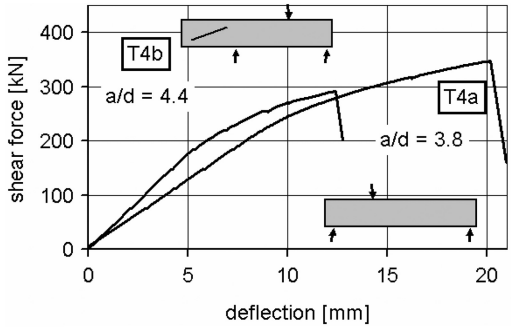

Figure 13. Comparison of the load bearing behavior with different shear slenderness, fiber ratio 0,9% p.v.

added to the concrete there was a significant increase in ultimate load. The load deflection curve indicates first cracks at approximate 220 kN, however, at this time no cracks were visible. Only at a higher load level capillary cracks with a spacing of appr. 3 mm appeared. About 90% of all cracks showed a width less than 0.05 mm and after failure these cracks were completely closed again and no longer visible.

The ultimate shear force of T4b with an enlarged shear slenderness of a/d = 4.4 was about 15% lower compared to T4a with a/d = 3.8 as presented in the diagram of figure 13. This leads to the assumption, that a higher arch action is still present even when a/d = 3.8. The different stiffness is not caused by the slenderness but the different spans of the first and second test set-ups. A comparison of T1b and T4a is not possible without restrictions, because they were fabricated with different casting methods. The fiber orientation, which is influenced by the casting method, will be investigated within the project.

4.3 *Results of the shear tests with openings*

Former shear tests from Hegger & Rauscher & Voss (2005) with multiple openings in the web showed that

Table 4. Results of the shear tests.

Test	$f_{c,cube100}$ [N/mm²] 3d	Day of test	$f_{ct,fl}$ [N/mm²]	V_u [kN]
T1a	88.9	151	22.7	234
T1b	88.9	174	21.2	267
T2a	86.8	134	12.3	134
T2b	86.8	134	12.3	147
T3a	103.2	162	23.1	abort
T3b	103.2	170	24.1	408
T4a	100.3	176	19.1	344
T4b	100.3	183	20.2	291
T6a	89.0	142	22.8	266
T6b	89.0	155	23.0	226
T7a	112.8	192	26.0	234
T7b	112.8	183	24.7	232

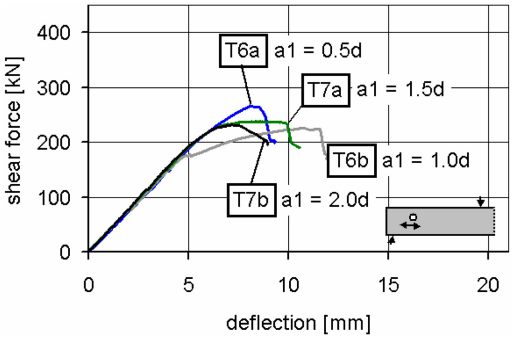

Figure 14. Comparison of the load bearing behavior with different spacings between support and single web opening.

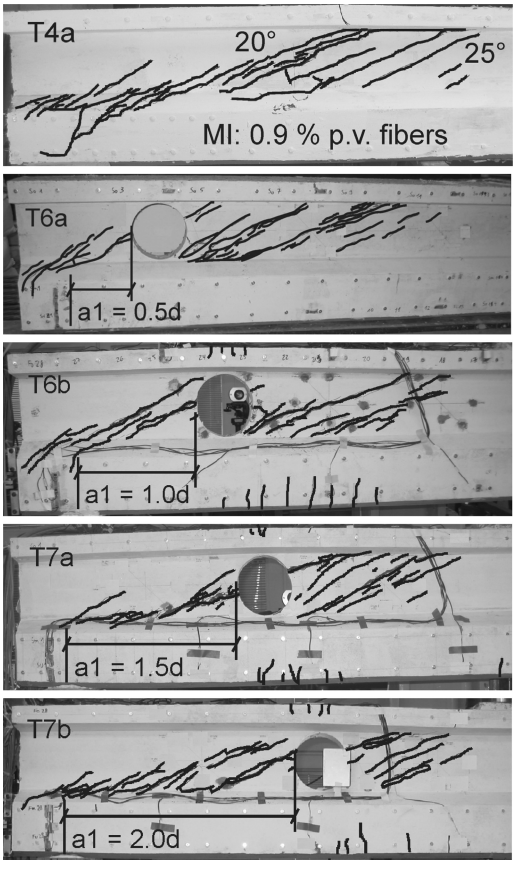

Figure 15. Comparison of the crack patterns with different spacings between support and single web opening.

the remaining shear resistance was about 60 to 65% compared to solid beams. Within the current research project the influence of single and multiple openings will be investigated systematically. Shear tests with single openings with different spacings to the support were already performed.

The load-deflection curves of tests with single openings with a diameter of d/2 are presented in figure 14. The best comparison to the solid beams is given by T4a, which had also a fiber ratio of 0.9% and a slenderness of a/d = 3.8. T1b with an ultimate shear force of 267 kN is not directly comparable because of different concreting methods.

All openings were arranged in the area, where the failure cracks of T4a appeared (figure 15). The opening of T6a was sufficiently close to the support, that the main part of the arch action was able to run underneath the opening. Nearly no loss of the initial stiffness was observed. In T6b the separation of a triangular part from the end of the beam to the opening has reduced the stiffness clearly. The loss of the effective depth led to a higher bending as indicated by several bending cracks at the bottom. The tests T7a and T7b showed bending cracks at the bottom as well but the separation of the triangle did not appear before failure. The cracks grew considerably towards the anchorage zone of the strands, especially in T7b. However a remarkable increase of the strand slip was not observed before failure.

4.4 *Outlook*

Girders with multiple web openings as well as girders with openings and additional shear reinforcement will follow and complete the experimental program of this research project. The presented model for the anchorage will be completed and calculation models for the shear resistance with and without openings will be derived. The authors acknowledge the support of the German Research Foundation.

REFERENCES

Bülte, S. 2008. Zum Verbundverhalten von Spannstahllitzen unter Betriebsbeanspruchung. Institute of Structural Concrete of Aachen University. Dissertation in progress

German Research Foundation. priority project (DFG SPP 1182). Nachhaltig Bauen mit UHPC (Sustainable Construction with UHPC)

Görtz, S. 2004. Schubrissverhalten von Stahlbeton- und Spannbetonbauteilen aus Normal- und Hochleistungsbeton. Dissertation. RWTH Aachen

Hegger, J. & Bertram, G. 2008a. Anchorage behavior of pretensioned strands in steel fiber reinforced UHPC. Proceedings, 2nd International Symposium on UHPC. Kassel. Germany

Hegger, J. & Bertram, G. 2008b. Shear carrying capacity of steel fiber reinforced UHPC. Proceedings, 2nd International Symposium on UHPC. Kassel. Germany

Hegger, J. & Rauscher, S. & Voss, S. 2005. Shear Carrying Capacity of Fiber-Reinforced UHPC. CCC° 2005. Lyon/Frankreich. pp. 1173–1180

Hegger, J. & Kommer, B. & Tuchlinski, D. 2006. Untersuchungen an Spannbetonträgern aus UHPC. Betonwerk + Fertigteil-Technik, BFT-China, pp. 3–8

Hoyer, E. 1939. Der Stahlsaitenbeton. Otto Elsner Verlagsgesellschaft. Berlin Wien Leipzig

Nitsch, A. 2001. Spannbetonfertigteile mit teilweiser Vorspannung aus hochfestem Beton. Dissertation. Institute of Structural Concrete of Aachen University. book 13. ISBN 3-9807302-0

Stocker, M.F. & Sozen, M.A. 1969. Bond characteristics of prestressed strand. Investigations of prestressed reinforced concrete of Highway bridges. University Illinois. Structural Research. Series No. 344

den Uijl, J. 1992. Bond and splitting action of prestressing strand. Proceedings. Bond in Concrete. Riga. S. 2/79-2/88